Effect of Support Structure in Au/Al_2O_3-TiO_2 Catalysts in Low-Temperature CO Oxidation

Maria Rajska[1,a], Piotr Długosz[2] and Rafał Zybała[3]

[1]*AGH University of Science and Technology, Faculty of Materials Science and Ceramic, Al. Mickiewicza 30, 30-059 Krakow, Poland*
[2]*Foundry Research Institute, Department of Non-Ferrous Metal Alloys, Zakopiańska 73, 30-418 Krakow, Poland*
[3]*Faculty of Materials Science and Engineering, Warsaw University of Technology, Wołoska 141, 02-507 Warsaw, Poland*

Abstract. The aim of this study was to determine the effect of the support phase composition (Al_2O_3–TiO_2) and the addition of gold on the catalytic properties in low-temperature CO oxidation. In this paper, the physicochemical properties and results of catalytic measurements performed for the obtained samples were investigated. The catalyst carriers were prepared using the sol-gel method with alkoxide $Al(C_3H_7O)_3$ and $Ti(C_3H_7O)_4$ employed to obtain the corresponding oxides, in the case of which the molar ratio (Al_2O_3:TiO_2) was 0.75:0.25, 0.50:0.50 and 0.25:0.75, thus corresponding to the molar ratio of the Al:Ti elements, i.e. 1.5:0.25, 2:1 and 0.5:0.75 respectively. The gold catalysts were prepared through the deposition of gold by the deposition precipitation method using the theoretical loading of Au 2 wt.%. To examine the effect of the phase composition on the catalytic activity of the obtained samples, appropriate carriers were calcined at two different temperatures: 500°C and 1350°C. This made it possible to obtain the intended polymorphs of aluminum oxide and titanium dioxide (γ–Al_2O_3, α–Al_2O_3, anatase and rutile). For certain samples, calcined at a high temperature, the aluminum titanium oxide (Al_2O_5Ti) phase was also observed. The prepared samples were characterized by XRD, BET, SEM, and additionally both particle size distribution analysis and measurements of the catalytic activity were performed. The highest catalytic activity was shown by Au/75Al–25Ti_LT, where T_{90} was about 110°C.

1 Introduction

The increased interest in nanometric materials observed in recent years caused the discovery of nanocrystalline gold, which proved to be a material with a high catalytic efficiency. The number of nano gold applications has continuously grown in the last few years and a great interest in gold in the nanometric form is still observable. Nanocrystalline gold is used in many reactions, including low temperature CO oxidation, H_2 synthesis in the presence of water vapor and carbon oxide (WGS - Water Gas Shift Reaction), and further purification of H_2 with CO for PEMs fuel cells (PROX - PReferential OXidation) [1-5]. The latest trend in the use of nano-sized gold focuses on creating hybrid materials used as various types of biosensors [6-8]. Devices like biosensors based on nano Au show a remarkably high sensitivity with high specificity. Another very interesting application is medicine and especially the rapid diagnosis of cancer or DNA damage [9-11]. Nano gold deposited on various support structures is also used for the selective oxidation of alkenes, alcohols, and even alkanes [12,13]. For nanomaterials, including oxides, a relationship between the size of the crystallite or grain powder and the exhibited surface free energy that is different for a nanopowder and a material with large grains was found. It was discovered that the less thermodynamically stable structure can be a stable substrate for the nano-sized metal particles through the reduction of the surface free energy. This relationship was studied for the first time for various crystalline phases of alumina (γ-Al_2O_3 and α-Al_2O_3) [14]. Similar research also focused on the polymorphic forms of TiO_2 [15,16].

The selection of an appropriate material to be used as a support is important for the preparation of catalysts with a high efficiency in CO oxidation, or oxidation of the volatile organic compounds [17]. Among the oxides used for oxidation there is titanium dioxide (anatase), which stabilizes the size of the nanoparticles of gold, thus preventing them from excessive expansion during heat treatment, and provides a uniform distribution of Au, and, in addition, participates in the oxidation of CO [18,19]. The effect of the TiO_2 phase was studied also in the case of the hydrogenation reaction [20,21]. Due to the crystal structure of TiO_2, it can be divided into three polymorph forms (anatase, brookite and rutile) having various structural and physical properties [22]. For catalytic applications, anatase is the most often used solution due to its semiconductor properties and inconsiderable defection from stoichiometry [23]. Anatase grains usually do not exceed 50 nm and are used in catalysis as adsorbents for organic compounds. Rutile grains are larger, usually exceeding 200 nm [24]. TiO_2 in the rutile form due to its stable structure allowing the use of higher temperatures,

[a] Corresponding author: rajska@agh.edu.pl

is used for instance in the catalytic oxidation of hydrogen chloride to chlorine [25]. Gold can be added to the catalytic system by various methods, including precipitation methods, sputtering or CVD, which enables obtaining Au particles <10 nm. However, the deposition - precipitation allows the most efficient preparation of highly active catalysts with Au sizes between 2 and 6 nm [26].

In this work, the effect of the phase composition of selected oxides (TiO_2 and Al_2O_3) and the addition of gold in the catalytic activity in response to the low temperature oxidation of CO was analyzed. In addition, the influence of the phase composition on the crystallite size of Au and the distribution of gold particles on the surface of the sample were determined.

2 Experimental

The samples were obtained by the sol-gel method, using the following, appropriately chosen alkoxides: aluminum and titanium ($Al(C_3H_7O)_3$, $Ti(C_3H_7O)_4$) (p.a., Avantor Performance Materials Poland S.A.) with a concentration of 1 M in anhydrous ethanol [27]. The alkoxides of aluminum and titanium were used for the preparation of the corresponding oxides, in the case of which the molar ratio (Al_2O_3:TiO_2) was determined to be 0.75:0.25; 0.50:0.50 and 0.25:0.75. After hydrolysis, the substrate precursors underwent aging for 2 days at room temperature and were subsequently dried at a temperature of 70°C for 24 hours. The samples for further study were calcined for 3 hours at two different temperatures: 500°C and 1350°C. A detailed description of the preparation of the catalyst carriers was described in the previous work [28]. This allowed obtaining the proper polymorphic phase of oxides, i.e. γ-Al_2O_3, α-Al_2O_3, anatase, rutile. Table 1 shows the composition of the outcome samples and their corresponding symbols.

Table 1. Symbols of samples.

Sample	Abbreviation	Sample	Abbreviation
$0.75Al_2O_3$-$0.25TiO_2$_500°C	75Al-25Ti_LT	Au/$0.75Al_2O_3$-$0.25TiO_2$_500°C	Au/75Al-25Ti_LT
$0.50Al_2O_3$-$0.50TiO_2$_500°C	50Al-50Ti_LT	Au/$0.50Al_2O_3$-$0.50TiO_2$_500°C	Au/50Al-50Ti_LT
$0.25Al_2O_3$-$0.75TiO_2$_500°C	25Al-75Ti_LT	Au/$0.25Al_2O_3$-$0.75TiO_2$_500°C	Au/25Al-75Ti_LT
$0.75Al_2O_3$-$0.25TiO_2$_1350°C	75Al-25Ti_HT	Au/$0.75Al_2O_3$-$0.25TiO_2$_1350°C	Au/75Al-25Ti_HT
$0.50Al_2O_3$-$0.50TiO_2$_1350°C	50Al-50Ti_HT	Au/$0.50Al_2O_3$-$0.50TiO_2$_1350°C	Au/50Al-50Ti_HT
$0.25Al_2O_3$-$0.75TiO_2$_1350°C	25Al-75Ti_HT	Au/$0.25Al_2O_3$-$0.75TiO_2$_1350°C	Au/25Al-75Ti_HT

All polymorphic forms of alumina above 1200°C are transformed into corundum. At temperatures higher than 1300°C, it is possible to obtain a permanent connection between corundum and rutile [29]. Rutile is a thermodynamically stable structure which is formed during the exothermic conversion of anatase in the temperature range of 500-1000°C, in the case of which the lower the transition temperature, the smaller the crystallites of TiO_2 [30,31]. The gold particles were deposited on the substrate by deposition precipitation to obtain 2% Au by weight in the final catalyst. A precursor of gold was chloroauric acid $HAuCl_4$ (p.a., Chempur) with a concentration of 0.088 M.

2.1 Methods

X-ray diffraction measurements were performed using the X'PERT Pro PANalytical diffractometer (CuKa radiation). The average crystallite size of gold was calculated using the Scherrer equation, and the quantitative phase composition of the samples calcined at 1350°C was calculated using the Rietveld method. For morphology observation, the samples calcined at 500°C were analyzed using the JEOL JSM 7500F scanning electron microscope, whereas for the observation of other samples (1350°C) a SEM NOVA NANO 200 scanning electron microscope from FEI was used. The studies of the particle size distribution were made employing the Malvern Mastersizer 2000. The measurements of the specific surface area of the samples were performed using the ASAP 2010 apparatus from Micromeritics Instrument Corporation.

2.2 Catalytic measurements

Catalytic tests were performed in a flow-through, quartz reactor connected with the quadrupole mass spectrometer (Thermostar QSD 300, BALZERS). The ionic currents were used to calculate the rate of conversion of CO to CO_2. Before the catalytic test, the samples (0.3 g) were standardized by their heating to 300°C under a constant air flow and kept at this temperature for 30 min. Catalytic investigations were performed in a gas flow of 100 cm^3h^{-1} in the temperature range from 25°C to 300°C. The reaction mixture contained 1 %vol. CO, 9 %vol. He, 17.8 %vol. O_2 and 72.2 %vol. N_2. Each catalytic measurement was repeated three times. For a better characterization of the catalytic activity, the temperature at which the conversion of CO to CO_2 was 50% (T_{50}) and 90% (T_{90}) was determined.

3 Results

3.1 XRD

The phase analysis of the samples calcined at 500°C showed that next to the crystalline phase was a certain amount of the amorphous phase. Reflections derived from TiO_2 correspond to the anatase phase (ICDD 01-073-1764). The reflections of crystalline Al_2O_3 were very extended and indicating the γ-Al_2O_3 phase (ICDD 00-010-0425) [32,33]. The XRD analysis of the samples with gold showed the large half-width reflections derived from the crystallites of gold (ICDD 04-003-5615) (Figure 1). The Au crystallite size was calculated from the Scherrer equation (see Table 2). The crystallite size of Au for samples was similar, i.e. 4 nm (Au/75Al-25Ti_LT, Au/25Al-75Ti_LT) and 5 nm (Au/50Al-50Ti_LT). This means that the difference in the phase composition in the sample does not significantly affect the size of the crystallites of gold. The calculated Au crystallite size of the samples calcined at a high temperature is frequently many times larger when compared to the same samples calcined at a lower temperature, D_{Au} = 50

nm (Au/75Al-25Ti_HT), D_{Au} = 57 nm (Au/50Al-50Ti_HT), D_{Au} = 97 nm (Au/25Al-75Ti_HT), (Figure 2). The gold crystallites of such large sizes no longer show catalytic properties. Their presence does not improve the catalytic effect for the whole system [1].

Table 2. Results of XRD and specific surface area measurements.

Sample	S_{BET} [m^2g^{-1}]	Crystallite size [nm]	Phase composition
75Al-25Ti_LT	339.01 ± 0,61	$D_{anatase}$ = 26 ± 1 $D_{\gamma\text{-}Al_2O_3}$ = 7 ± 1	TiO_2-anatase, γ-Al_2O_3
50Al-50Ti_LT	227.70 ± 1.79	$D_{anatase}$ = 29 ± 1 $D_{\gamma\text{-}Al_2O_3}$ = 8 ± 1	TiO_2-anatase, γ-Al_2O_3
25Al-75Ti_LT	284.79 ± 0.87	$D_{anatase}$ = 30 ± 1 $D_{\gamma\text{-}Al_2O_3}$ = 8 ± 1	TiO_2-anatase, γ-Al_2O_3
Au/75Al-25Ti_LT	346.26 ± 1.29	$D_{anatase}$ = 23 ± 1 $D_{\gamma\text{-}Al_2O_3}$ = 6 ± 1 D_{Au} = 4 ± 1	TiO_2-anatase, γ-Al_2O_3, Au
Au/50Al-50Ti_LT	288.37 ± 0.88	$D_{anatase}$ = 26 ± 1 $D_{\gamma\text{-}Al_2O_3}$ = 7 ± 1 D_{Au} = 5 ± 1	TiO_2-anatase, γ-Al_2O_3, Au
Au/25Al-75Ti_LT	305.76 ± 0.59	$D_{anatase}$ = 25 ± 1 $D_{\gamma\text{-}Al_2O_3}$ = 7 ± 1 D_{Au} = 4 ± 1	TiO_2-anatase, γ-Al_2O_3, Au
75Al-25Ti_HT	0.73 ± 0.05	D_{rutile} = 126 ± 1 $D_{\alpha\text{-}Al_2O_3}$ = 108 ± 1	TiO_2-rutile, α-Al_2O_3
50Al-50Ti_HT	1.29 ± 0.01	D_{rutile} = 129 ± 1 $D_{\alpha\text{-}Al_2O_3}$ = 108 ± 1 $D_{Al_2O_5Ti}$ = 126 ± 1	TiO_2-rutile, α-Al_2O_3 Al_2O_5Ti
25Al-75Ti_HT	1.60 ± 0.01	D_{rutile} = 138 ± 1 $D_{\alpha\text{-}Al_2O_3}$ = 122 ± 1 $D_{Al_2O_5Ti}$ = 180 ± 1	TiO_2-rutile, α-Al_2O_3 Al_2O_5Ti
Au/75Al-25Ti_HT	2.40 ± 0.01	D_{rutile} = 126 ± 1 $D_{\alpha\text{-}Al_2O_3}$ = 107 ± 1 D_{Au} = 50 ± 1	TiO_2-rutile, α-Al_2O_3, Au
Au/50Al-50Ti_HT	1.19 ± 0.02	D_{rutile} = 129 ± 1 $D_{\alpha\text{-}Al_2O_3}$ = 108 ± 1 $D_{Al_2O_5Ti}$ = 126 ± 1 D_{Au} = 57 ± 1	TiO_2-rutile, α-Al_2O_3, Al_2O_5Ti, Au
Au/25Al-75Ti_HT	1.68 ± 0.01	D_{rutile} = 137 ± 1 $D_{\alpha\text{-}Al_2O_3}$ = 123 ± 1 $D_{Al_2O_5Ti}$ = 180 ± 1 D_{Au} = 97 ± 1	TiO_2-rutile, α-Al_2O_3, Al_2O_5Ti, Au

For sample 75Al-25Ti_HT corundum (ICDD 04-007-9906) was 92.1 wt.% and rutile was 7.9 wt.% (ICDD 04-007-5987). In sample 50Al-50Ti_HT corundum was 48.4 wt.%, rutile 7.4 wt.% and a new phase aluminium titanium oxide of 44.2 wt.% appeared (ICDD 00-041-0258). In sample 25Al-75Ti_HT corundum was 40.3 wt.%, rutile 31.3 wt.% and aluminium titanium oxide 28.4 wt.%. A new phase containing aluminum and titanium was observed for the samples with a high ratio of titanium to aluminum, i.e. for sample 50Al-50Ti_HT where the Al:Ti molar ratio is 2:1, and for sample 25Al-75Ti_HT where the Al:Ti molar ratio is 0.5:0.75. For sample 75Al25Ti_HT the theoretical weight percent of titanium is 12%, for sample 50Al-50Ti_HT it is already 28 wt.% and 61 wt.% for sample 25Al75Ti_HT.

The calculated content of the new phase (Al_2O_5Ti) shows that it rises in the first place at the expense of decreasing the amount of rutile. The losses of the α-Al_2O_3 phase appear to be larger, but in fact, they are strongly correlated with predefined stoichiometry and the stoichiometry of the new phase.

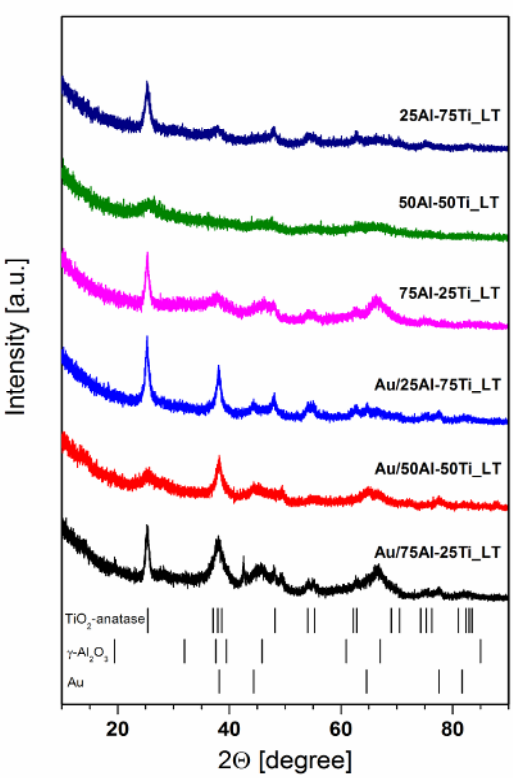

Figure 1. X-ray diffraction patterns of samples calcined at a low temperature.

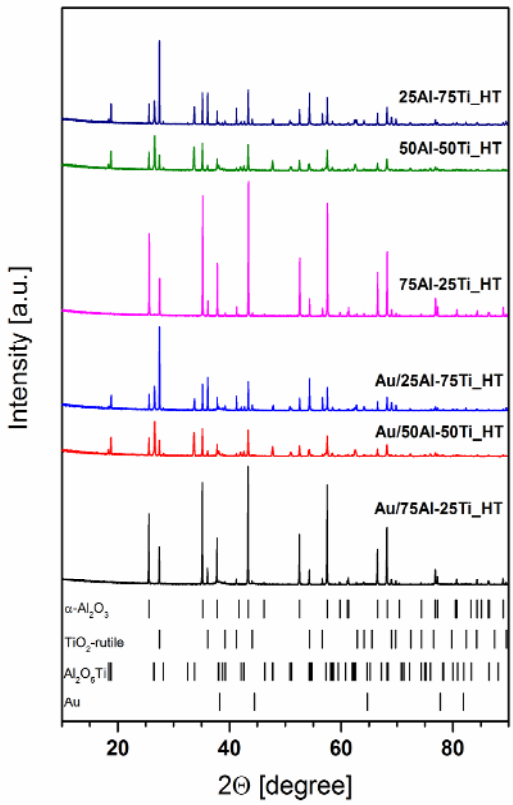

Figure 2. X-ray diffraction patterns of samples calcined at a high temperature.

The phase composition of the samples after the gold addition was not changed. A share of Au in the sum of the oxides was 1.5 by weight for Au/75Al-25Ti_HT, for Au/50Al-50Ti_HT it equalled 1.3 wt.% and for Au/25Al-75Ti_HT it reached 1.3 wt.%. The planned gold content is lower than the one obtained, i.e. 2 %wt., which is still within the optimum range of the Au content for this type of a catalyst [19].

3.2 Particle size distribution

The analysis of particle size distribution expressed as volume and quantity percentage indicates that the grains of powder form agglomerates. Most of the particles are between 0.3 and 10 microns; however, this distribution is changed after the gold addition (Figure 3 and Figure 4).

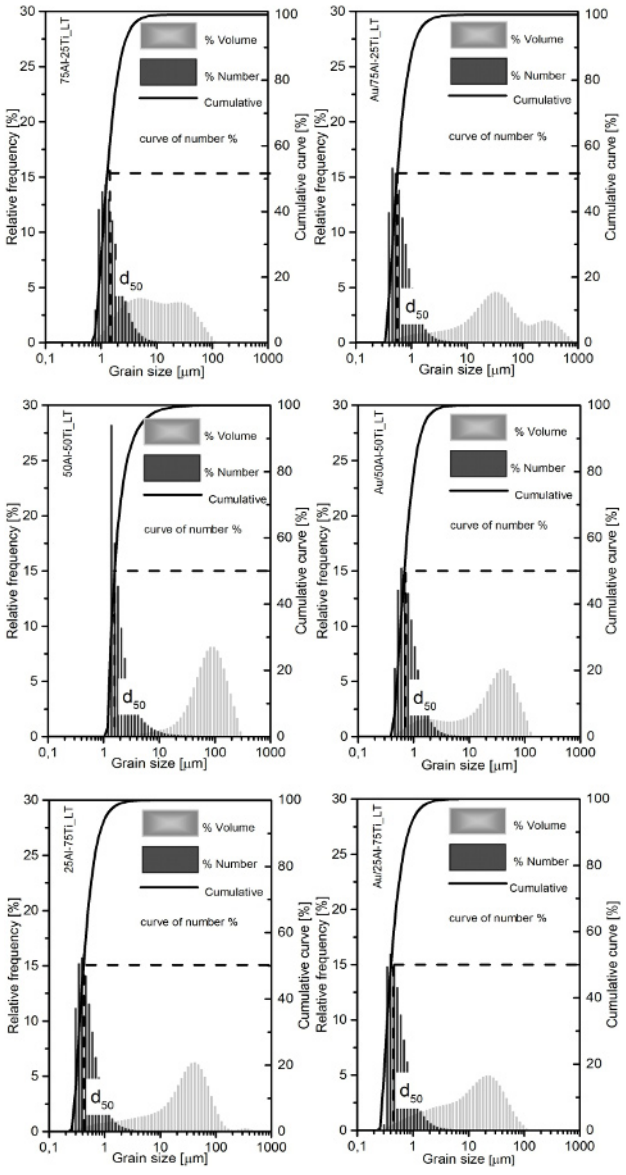

Figure 3. Grains distribution for samples calcined at a low temperature.

The average particle size of sample 75Al-25Ti_LT was 1.26 μm and after the application of Au it was reduced to 0.55 microns. For sample 50Al-50Ti_LT the average particle size was 1.55 μm and after gold deposition it was 0.68 μm. The situation was found to be similar for sample 25Al-75Ti_LT, for which the average grain size was 0.45 μm and 0.39 μm after the application of gold. In the case of samples 75Al-25Ti_LT and 50Al-50Ti_LT the average particle size was 2.3 times lower, and in the case of sample 25Al-75Ti_LT it was 1.15 times lower.

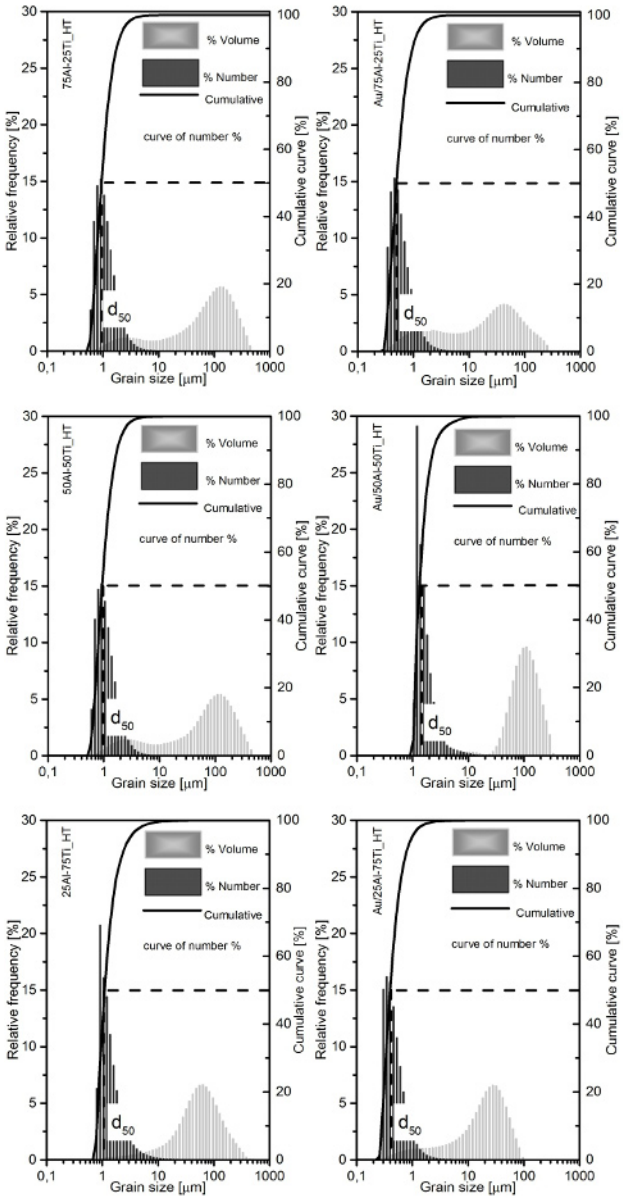

Figure 4. Grains distribution for samples calcined at a high temperature.

It was observed that the particle size was reduced and simultaneously the specific surface area increased. For samples 75Al-25Ti_LT, 50Al-50Ti_LT and 25Al-75Ti_LT the specific surface area was 339.01 m^2g^{-1} 227.70 m^2g^{-1}, 284.79 m^2g^{-1} respectively and increased to 346.26 m^2g^{-1}, 288.37 m^2g^{-1} and 305.76 m^2g^{-1}. The increase may be associated with the disintegration of agglomeration during the gold deposition-precipitation procedure. It is also probable that in the case of the sample containing γ-Al_2O_3 partial dissolving of a quantity of alumina which then recrystallized again could have taken place[34].

Similarly, changes occur in the case of the samples calcined at a higher temperature. For 75Al-25Ti_HT the mean grain size was 0.96 μm and after the addition of

gold it reached 0.53 µm. The average grain size for samples 50Al-50Ti_HT and 25Al-75Ti_HT was 0.89 µm and 1.03 µm, whereas after gold deposition it changed to 1.35 µm and 0.39 µm respectively. For the samples calcined at a high temperature, after the application of gold the average particle size generally decreases: 1.8 times for sample Au/75Al-25Ti_HT and 3.5 times for sample Au/25Al-75Ti_HT. The only exception was sample Au/50Al-50Ti_HT with a small increase in the average particle size, suggesting that the effect of the addition of gold outweighs the potential effect of the disintegration of powder agglomerates. These results are in line with the measurements of the specific surface area showing that after the addition of gold the specific surface area increased for Au/75Al-25Ti_HT (0.73 m^2g^{-1} to 2.40 m^2g^{-1}) and Au/25Al-75Ti_HT (1.60 m^2g^{-1} to 1.68 m^2g^{-1}) and decreased for Au/50Al-50Ti_HT (1.29 m^2g^{-1} to 1.19 m^2g^{-1}).

The decrease in the specific surface area after Au deposition, described in the literature, was observed for the samples the carriers of which were calcined at 1350°C [18]. This effect is noticeable for samples coming from the carriers calcined at low temperatures. This could be most likely due to the dominant effect of the disintegration of agglomerates.

3.3 SEM

Grains of the carriers and the gold catalysts are presented in the micrographs shown in Figure 5 and Figure 6. All samples have irregular shapes and form agglomerates with different sizes. For the samples calcined at 500°C, agglomerates have a size of about 0.5 micron and for the samples calcined at higher temperatures agglomerates measure about a few microns. After the gold addition the carrier grains were smaller, which can be associated with the disintegration of the agglomerates presented in the beginning and secondly, the partial recrystallization of γ-Al_2O_3 which could have been possible for a sample calcined at a lower temperature (see Figure 5). In aqueous systems, γ-Al_2O_3 can again be transformed into aluminum hydroxide or aluminum oxyhydroxide, when the final heat treatment re-creates γ-Al_2O_3, but with a high specific surface area [35].

The distribution of the gold particles on the surface is uniform. For sample Au/75Al-25Ti_LT the gold particles have a small size, reaching about 10 nm (D_{Au} = 5 nm – XRD) (Figure 5).

As a result of the exothermic phase transition of γ-Al_2O_3 to corundum one observes the loss of porosity and reduction in the specific surface area as well as an increase in the grain size. α-Al_2O_3 powder has a specific surface area (S_{BET}) of less than 1 m^2g^{-1} and a micropore volume of less than 0.5 cm^3g^{-1}. It is also possible to obtain the polymorph of the aluminum oxide specific surface area of 66 m^2g^{-1} for decomposition and calcination of α-$Al(OH)_3$ at 530°C [36]. After Au deposition, the grains of the samples (from the carriers calcined at high temperature) did not show significant deformation or there was no reduction in the size of the agglomerates. The observed Au particles were evenly distributed over the surface of the sample.

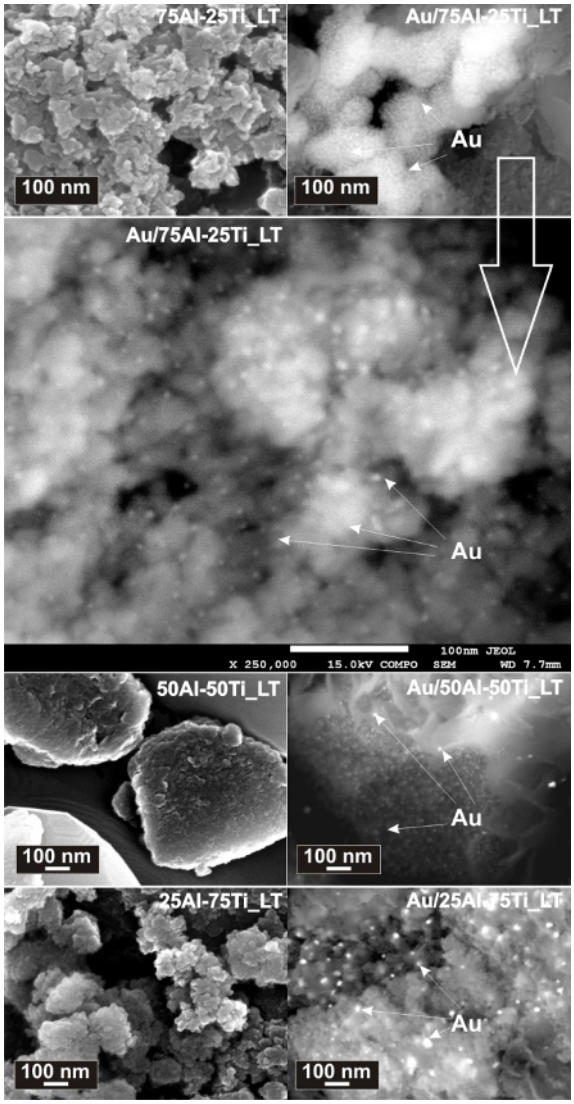

Figure 5. SEM images of the support and the gold supported catalysts for samples calcined at a low temperature.

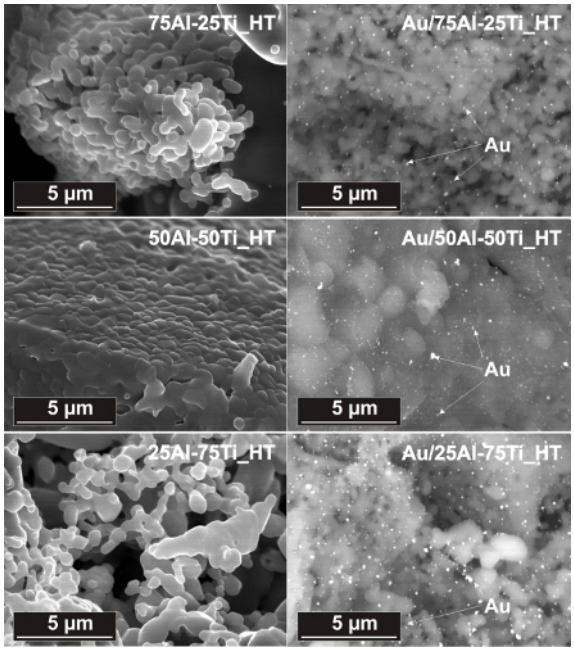

Figure 6. SEM images of the support and gold supported catalysts for samples calcined at a high temperature.

The average size of the gold particles determined from the microimages of sample Au/75Al-25Ti_HT was 80 nm (Figure 6). This is a value close to the result calculated by the Scherrer equation (D_{Au} = 50 nm). For the remaining samples and based on the microphotographs, the Au particles have the calculated size of 85 nm for Au/50Al-50Ti_HT (D_{Au} = 54 nm – XRD) and 110 nm for Au/25Al-75Ti_HT (D_{Au} = 97 nm – XRD).

3.4 Catalytic tests

The catalytic activity of the obtained carriers and Au/catalysts was determined on the basis of the following oxidation reaction of carbon monoxide: $2CO + O_2 \rightarrow 2CO_2$.

The CO oxidation test was carried out in the 25-300°C temperature range due to the fact that above a temperature of 320°C the phenomenon entailing the sintering of gold crystallites takes place, which results in a significant increase in their size and thus a loss of their catalytic properties [1]. For the samples that do not contain gold it can be observed that the carriers calcined at a higher temperature had better catalytic properties than the samples with gold (Figure 7).

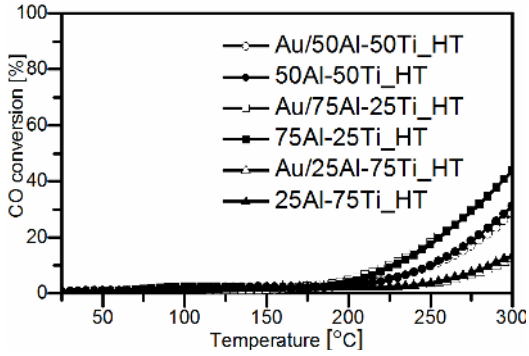

Figure 7. CO conversion for samples calcinated at high temperature.

This is probably related to the phase composition of the sample, i.e. the presence of the following phases: α-Al_2O_3 and TiO_2-rutile, especially when taking into account that a specific surface area for this material is small (about 0.3 m^2g^{-1}). The efficiencies of the system (30% conversion of CO) are still unsatisfactory from the point of view of its using as a catalyst in the low temperature oxidation of CO. After the gold addition, changes in the efficiency of the tested samples were observed.

The highest conversion rate of CO to CO_2 was obtained for sample Au/75Al-25Ti_HT, for which at a temperature of 300°C conversion reached about 35%. In this case, there were no positive changes when adding gold to the system. The calculated degree of conversion of the CO for media is low with respect to the systems containing gold in the low temperature range (Figure 8). The presence of gold brings a significant improvement in the catalytic properties of the samples calcined at a lower temperature. The CO oxidation reaction began at about 30°C for all samples and 90% conversion of CO to CO_2 was achieved at a temperature of about 110°C (Au/75Al-25Ti_LT), as shown in Table 3. The best carrier was sample 50Al-50Ti_LT with CO conversion similar to the conversion of 75Al-25Ti_HT. With a decrease in the percentage of the titanium dioxide degree, the conversion of CO (T_{50} and T_{90}) is moved towards lower temperatures.

Table 3. Temperatures of 50% CO conversion and 90% CO conversion.

Sample	T_{50} [°C]	T_{90} [°C]
Au/75Al-25Ti_LT	65	110
Au/50Al-50Ti_LT	100	155
Au/25Al-75Ti_LT	120	200
Au/75Al-25Ti_HT	>300	-
Au/50Al-50Ti_HT	>300	-
Au/25Al-75Ti_HT	>300	-

For the best sample (Au/75Al-25Ti_LT) lowering of the temperature at which the system shows a complete CO conversion from the high temperature range (>300°C) to the low temperature range (>110°C) was observed. This would mean that in the test reaction, a dominant role in obtaining a high catalytic activity for CO oxidation is played by the crystallite size of gold. For samples characterized by a high efficiency of CO oxidation, gold crystallites have a size of about 4 nm. The samples which are obtained from the carrier calcined at high temperatures have large gold crystallites (D_{Au} = 50 nm, D_{Au} = 57 nm, D_{Au} = 97 nm). Gold of this size does not exhibit catalytic properties.

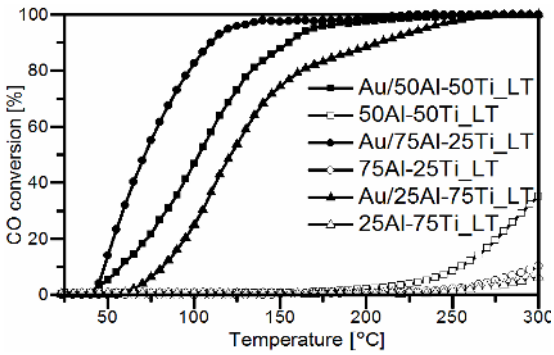

Figure 8. CO conversion for samples calcined at a low temperature.

Summary

The study is an attempt to explain the change in the catalytic activity in low-temperature CO oxidation, depending on the presence of different polymorphic forms of the base material. These research works led to the conclusion that the catalytic activity of this reaction is very intense for the catalysts in which there is TiO_2, which is in the form of anatase. For analogous systems containing rutile the catalytic activity was reported to be very low (T_{50}>300°C) and not depending on whether the sample with gold or a pure carrier was analyzed. The phase composition of the substrate significantly affects the size of the crystallites of gold and stabilizes their growth, thus significantly influencing the high catalytic activity

of the samples the carriers of which were calcined at a low temperature. The size of gold crystallites was calculated using the Scherrer equation and was within the following two size ranges, i.e:4 to 5 nm and from 50 to 97 nm. Sample Au/75Al-25Ti_LT has the best catalytic activity . Samples, the carriers of which were calcined at a high temperature, were characterized by a low specific surface area. They contained α-Al_2O_3 and rutile and did not create proper conditions for the deposition of the gold particles of a nanometric size. The nanometer-sized gold is necessary to obtain the high catalytic activity in a low temperature CO oxidation reaction.

Acknowledgment

M. Rajska acknowledges the Statutory Project for Science (Grant for Young Scientists no.15.11.160.763) 2015 at the Department of Inorganic Chemistry, Faculty of Materials Science and Ceramics, AGH UST.
This work has been partially financed as a research project no. DEC-2014/12/S/ST8/00582 from the resources assigned to science by National Science Centre (NCN, Poland) and the National Centre for Research and Development (NCBR, Poland) under the project no. PBS3/A5/49/2015.

References

1. G.C. Bond, D.T. Thompson, Gold Bull. **33**, 41 (2000)
2. G.C. Bond, C. Louis, D.T. Thompson *Catalysis by Gold, Catalytic Science Series – Vol.6* (Imperial College Press, London 2006)
3. V.G. Milt, S. Ivanova, O. Sanz, M.I. Domínguez, A. Corrales, J.A. Odriozola, M.A. Centeno, Appl. Surf. Sci. **270**, 169 (2013)
4. A.T. Miah, B. Malakar, P. Saikia, Catal. Lett. **146**, 291 (2016)
5. T. Montini, M. Monai, A. Betram, I. Romero-Ocaña, P. Fornasiero, Mat. Sci. Semicon. Proc. **42**, 122 (2016)
6. J.E. Kim, J.H. Choi, M. Colas, D.H. Kim, H. Lee, Biosens. Bioelectron. **80**, 543, (2016)
7. Y.-M. Cheng, H.-B. Fa, W. Yin, C.-J. Hou, D.-Q.Huo, F.-M. Liu, Y. Zhang, C. Chen, J. Solid State Electrochem. **20**, 327 (2016)
8. W. Ma, L. Xu, L. Wang, H. Kuang, C. Xu, Biosns. Bioelectron. **79**, 220 (2016)
9. A. Barbasz, M. Oćwieja, J. Exp. Nanosci. **11**, 564 (2016)
10. J.H. Myung, K.A. Tam, S.-J. Park, A. Cha, S. Hong, WIREs. Nanomed. Nanobi. **8**, 223 (2016)
11. Y.-P. Kim, H.-S. Kim, Chembiochem, **17**, 275 (2016)
12. S. Rautiainen, O. Simakova, H. Guo, A.-R. Leino, K. Kordás, D. Murzin, M. Leskelä, T. Repo., Appl. Catal. A: Gen. **485**, 202 (2014)
13. P.-L. Zhu, X.-Y. Tang, M. Shi, Chemistry Open, **5**, 33 (2016)
14. J.M. McHale, A. Auroux, A.J. Perrott, A. Navrotsky, Science **277**, 788 (1997)
15. H. Zhang, B. Chen, J.F. Banfield, Phys. Chem. Chem. Phys. 11, 2553 (2009)
16. [c] S.-G. Shang, X. Li, L. Zhao, R. Lu, H.-F. Chen, Mater. Sci. Forum **852**, 238 (2016)
17. M. Hosseini, S. Siffert, H.L. Tidahy, R. Cousin, J.-F. Lamonier, A. Aboukais, A. Vantomme, M. Roussel, B.-L. Su, Catal. Today **122**, 391 (2007)
18. W.-C. Li, M. Comotti, F. Schüth, J. Catal. **237**, 190 (2006)
19. M.M. Schubert, S. Hackemberg, A.C. van Veen, M. Muhler, V. Plzak, R.J. Behm, J. Catal. **197**, 113 (2001)
20. Y. Li, B. Xu, Y. Fan, N. Feng, A. Qiu, J.M.J. He, H. Yang, Y. Chen, J. Mol. Catal. A: Chem. **216**, 107 (2004)
21. [B] X.-Z. Ding, X.-H. Liu, Y.-Z. He, J. Mater. Sci. Lett. **15**, 1789 (1996)
22. H. Iida, A. Igarashi, Appl. Catal. A: Gen. **298**, 152 (2006)
23. J.A. Moma, M.S. Scurrell, W.A. Jordaan, Top. Catal. **44**, 167 (2007)
24. M.Y. Kang, H.J. Yun, S. Yu, W. Kim, N.D. Kim, J. Yi, J. Mol. Catal. A: Chem. **368– 369**, 72 (2013)
25. K. Seki, Catal. Surv. Asia 14, 168 (2010)
26. G.C. Bond, D.T. Thompson, Catal. Rev.- Sci. Eng. **41**, 319 (1999)
27. D.A.H. Hanaor, I. Chironi, I. Karatchevtseva, G. Triani, C.C. Sorrell, Adv. Appl. Ceram. **111**, 149 (2012)
28. L.L. Hong, Y.J. Jong, M.L. Hyung, J. Mat. Sci. **32**, 5687 (1997)
29. M. Rajska, Materiały Ceramiczne/Ceramic Materials **67**, 393 (2015)
30. [A] J.M. Low, B. Curtain, M. Phillips, Z.Q. Liu, M. Ionescu, J. Aust. Ceram. Soc. **48**, 198 (2012)
31. [AA] J. Li, L. Liu, T.-K. Sham, Chem. Mater. **27**, 3021 (2015)
32. [D] S.R. Kumar, S.C. Pillai, U.S. Hareesh, P. Mukundan, K.G.K. Warrier, Mater. Lett. **43**, 286 (2000)
33. [E] R. Janes, L.J. Knightley, Dyes Pigm. **56**, 11 (2003)
34. L. Samain, A. Jaworski, M. Edén, D.M. Ladd, D.-K. Seo, F.J. Garcia-Garcia, U. Häussermann, J. Solid State Chem. 217, 1 (2014)
35. A.A. Tsyganenko, P.P. Mardilovich, J. Chem. Soc., Faraday Trans. **92**, 4843 (1996)
36. T. Tsuchida, Solid State Ionics **63–65**, 464 (1993)